Validation of quantitative Ronchi test through numerical propagation

Sukmock Lee[1,*] and Manuel Guizar-Sicairos[2,3]

[1]*Department of Physics, Inha University, Incheon, 402-751, Republic of Korea*
[2]*The Institute of Optics, University of Rochester, Rochester, 14627, New York, USA*
[3]*Current address: Paul Scherrer Institut, CH-5232 Villigen PSI, Switzerland*
** smlee@inha.ac.kr*

Abstract: We validate the quantitative analysis of Ronchigrams for wavefront sensing through detailed numerical simulations. Analysis of the experimental Ronchigrams provides the wavefront aberrations, the F/# of the beam and the distance of the Ronchi ruling from the paraxial focus. These retrieved parameters are used to numerically simulate the Ronchigrams with excellent agreement. This favorable comparison validates the accuracy of the wavefront recovery and provides a tool to examine the accuracy and robustness of this wavefront measurement technique.

OCIS codes: (120.5050) Phase measurement; (100.5070) Phase retrieval

References and links

1. J. R. Fienup, "Phase-retrieval algorithms for a complicated optical system," Appl. Opt. **32**(10), 1737 (1993).
2. M. Guizar-Sicairos, and J. R. Fienup, "Measurement of coherent x-ray focused beams by phase retrieval with transverse translation diversity," Opt. Express **17**(4), 2670–2685 (2009).
3. G. R. Brady, and J. R. Fienup, "Nonlinear optimization algorithm for retrieving the full complex pupil function," Opt. Express **14**(2), 474–486 (2006).
4. S. Lee, and J. Sasian, "Ronchigram quantification via a non-complementary dark-space effect," Opt. Express **17**(3), 1854–1858 (2009).
5. V. Ronchi, "Forty Years of History of a Grating Interferometer," Appl. Opt. **3**(4), 437–451 (1964).
6. T. Yatagai, "Fringe scanning Ronchi test for aspherical surfaces," Appl. Opt. **23**(20), 3676–3679 (1984).
7. S. Lee, "Direct determination of f-number by using Ronchi test," Opt. Express **17**(7), 5107–5111 (2009).
8. J. Jeong, B. Lee, and S. Lee, "Determination of paraxial image plane location by using Ronchi test," Opt. Express. **18**(17) 18249-18253 (2010).
9. There are many different conventions, but we followed the one in J. C. Wyant and K. Creath, "Basic Wavefront Aberration Theory for Optical Metrology," in *Applied Optics and Optical Engineering*, XI, 1992, Academic Press, Inc.
10. J. W. Goodman, *Introduction to Fourier Optics, 3rd Ed.* (Roberts & Company, Englewood, 2005).
11. D. Malacara, *Optical Shop Testing*, 2nd Ed., Ch. 9 (A Wiley-Interscience Publication, 1992).

1. Introduction

Phase retrieval can be used to determine the aberrated wavefront (optical field) without the need of calibrated interferometers or wavefront sensors. This iterative approach is based on matching the measured point spread functions (PSFs) with a numerical model of the field digitally propagated through the optical system. The relationship between the optical field in the entrance pupil and the optical field at the detector plane can be fairly accurately modeled using Fourier (or Fresnel) transforms if the system is paraxial. Phase retrieval thus has been used in a variety of applications, such as optical wavefront sensing [1] and characterization of focused coherent x-ray beams. By either perturbing the field with a moveable structure [2] or collecting wavefront images at several planes near focus [3], the success rate of phase retrieval has been increased significantly. These additional measurements have experimental similarities to those required for a recently developed quantitative Ronchi test [4]. For this test, Ronchigrams are measured with the binary Ronchi ruling at different transverse positions and orientations. This set of Ronchigrams allows quantitative determination of the transverse ray aberrations over the whole pupil [4].

#129106 - $15.00 USD Received 27 May 2010; revised 10 Aug 2010; accepted 10 Aug 2010; published 16 Aug 2010

Conventional Ronchi test with a binary ruling is one of the simplest methods used for evaluating aberrations qualitatively [5] and there have been several trials to render it quantitative method. T. Yatagai, for example, applied the synchronuous phase detection method to Ronchi test for aspherical surfaces [6], in which a binary ruling was moved stepwise a number of times sideways to achieve the first derivatives of the wavefront by assuming the ruling at the paraxial focus. However, in order to convert the measurement of the derivatives of the wavefront into the wavefront aberration, the *f*-number of the system must be given *a priori*. In addition, even though it is easy to assume the location of the ruling at the paraxial focus to develop an analytic formula, but it is not trivial to accurately locate the paraxial focus of an aberrated beam in an experimental setup. To our best knowledge, Ronchi test have been failed to implement the effect of the ruling at different locations. Recently we have demonstrated that by measuring the aberrations with a ruling at different longitudinal positions with respect to the paraxial focal point, it is possible to determine the *f*-number [7] and the location of paraxial focus [8], which renders the Ronchi test a self-consistent wavefront sensing tool.

To validate the Ronchi test from a physical optics point of view, and to show the sensitivity of Ronchigrams at different locations of ruling, we developed a program to generate numerically simulated Ronchigrams. For the simulations we used the values of several experimental parameters that are directly determined by the quantitative Ronchi test, including the measured aberrations. By comparing the corresponding Ronchigrams at several different locations of the ruling, we observed a great agreement between the experimental and the simulated Ronchigrams. This indicates the accuracy of the aberrations determined by the Ronchi test as well as a validity of the developed numerical simulation.

2. Experiments and results

The experimental layout of the Ronchi test is shown in Fig. 1. The aperture of diameter 25 mm is placed 389 mm to the right of a 5 μm diameter pinhole which is illuminated with a focused Helium-Neon laser beam of 632.8 nm wavelength. The first surface of the lens is fixed 4 mm to the right of the aperture to within an accuracy of ±0.5 mm. A binary Ronchi ruling of 200 μm period was placed in the path of the beam, near the paraxial image plane. A plano-convex lens with focal length 25 mm was used as an imaging lens to relay the exit pupil of the system to the detector surface. Each frame was 640 by 512 pixels and the detector pixel pitch was 10.4 μm. For data acquisition, the vertical Ronchi ruling is translated by half a period to measure complementary Ronchigrams (0-phase and π-phase), then these measurements are repeated with the ruling oriented horizontally.

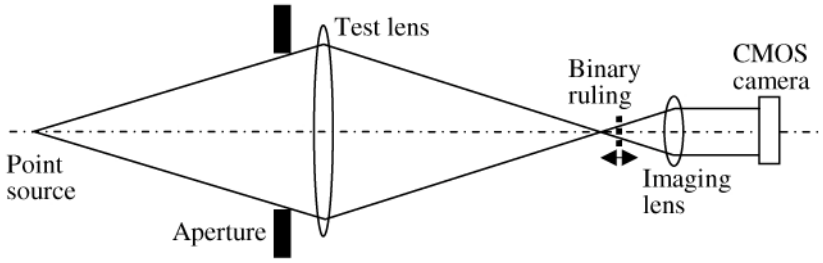

Fig. 1. Ronchi test setup for measuring transverse ray aberrations in a beam.

This procedure is then repeated with the ruling at various longitudinal positions near the paraxial image, which allows us to retrieve the F/# and ruling locations with respect to the paraxial image plane as well as the wavefront aberrations. The ruling is mounted on a translation stage having a precision of 2 μm and translated (along the beam propagation direction) to 5 different locations separated by 0.50 mm. The distance of the ruling with respect to the test lens or the paraxial image plane are not known *a priori* but are determined when a full data analysis is performed. To achieve the image quality for the analysis, the

#129106 - $15.00 USD Received 27 May 2010; revised 10 Aug 2010; accepted 10 Aug 2010; published 16 Aug 2010

intensity uniformity was checked as a prerequisite and found to be uniform enough to analyze Ronchigrams

Figures 2(a) thru 2(e) show the π-phase Ronchigrams [4] with a vertical ruling as a function of translation stage location. By combining the complementary 0-phase images, which are measured with the ruling shifted laterally by a half period of the ruling, and the two equivalent images with the horizontal ruling, we determined 35 Zernike polynomial coefficients that describe the pupil wavefront [9]. Among these, a full list of third-order aberrations at various locations is listed in Table 1. Figure 3 shows the two dominant Zernike polynomial coefficients as a function of the longitudinal position of the ruling. These wavefront aberrations were estimated using F/# = 5.24, which was obtained also from the Ronchigram analysis [7]. While the third-order spherical aberration a_8 is constant within the experimental error that is described below, the defocus aberration a_3 is linearly proportional to the longitudinal location. All other coefficients as well as other third-order coefficients, except a_6 (coma), were determined to be 0.1 waves or less in magnitude. The dependence of the coefficient a_6 on the location is believed to be due to the slight misalignment of the setup, even though the alignment was carefully done, which can be seen as slight asymmetries in Ronchigrams. In contrast, the linear dependence of the coefficient a_3 on the location is due to the displacement of the image plane with respect to the paraxial image plane and it is used to determine the *f*-number [7] and the paraxial image point location.

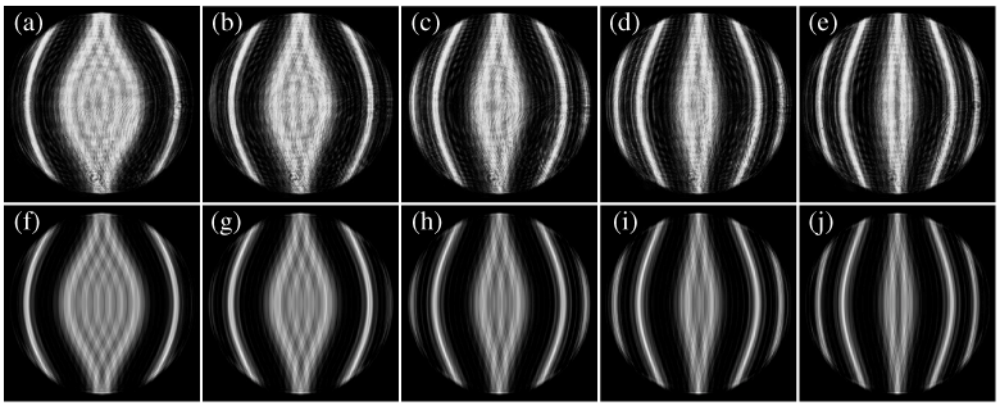

Fig. 2. π-phase Ronchigrams with vertical ruling at (a) 13.00, (b) 13.50, (c) 14.00, (d) 14.50, and (e) 15.00 mm of the longitudinal translation stage and (f) thru (j) are their corresponding simulated images. All images are cropped to 512 by 512 pixels from the original sizes.

Table 1. Third-order aberrations at various locations in unit of waves [7].

Locations (mm)	13.00	13.50	14.00	14.50	15.00
a_3	6.77	8.53	10.27	12.10	13.95
a_4	0.00	–0.08	–0.02	–0.01	–0.02
a_5	0.02	0.00	–0.00	–0.01	–0.01
a_6	–0.34	–0.26	–0.19	–0.14	–0.12
a_7	–0.08	–0.06	0.02	0.04	0.04
a_8	2.08	2.21	2.14	2.18	2.21

#129106 - $15.00 USD Received 27 May 2010; revised 10 Aug 2010; accepted 10 Aug 2010; published 16 Aug 2010

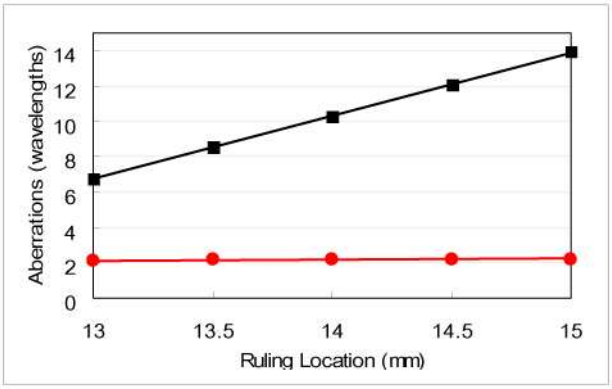

Fig. 3. Defocus $a3$ (squares) and spherical aberration $a8$ (circles) as a function of ruling's longitudinal position. The accompanied lines are the fitted lines. These values were determined by the quantitative Ronchigram analysis using F/# = 5.24, as retrieved from the data.

In order to determine the location of the ruling used with respect to the paraxial image plane, the data of the defocus aberration a_3 in Fig. 3 was fitted to a straight line by using the method described in [8]. The best fit equation of the line is $a_3 = 3.589z - 39.924$, where a_3 is in units of waves and z is the location of the ruling in units of mm. At the paraxial image plane, where no defocus wavefront aberration is assumed, the two polynomial coefficients must be related by $a_3=3a_8$ within the 3rd-order aberration theory, because the corresponding two Zernike polynomials are given as $z_3 = 2\rho^2 - 1$ and $z_8 = 6\rho^4 - 6\rho^2 + 1$, respectively, where ρ is the reduced radial coordinate for the pupil [9]. Thus the location of paraxial image plane can be obtained by solving the equation, $z_{PIP} = (3a_8+39.924)/3.589$ with the determined primary spherical aberration a_8 being 2.16±0.06 waves. While the ruling location's uncertainty is 0.002 mm, the uncertainty for the aberrations is assumed to be 5% over the whole procedure. The solution, 12.93±0.05 mm, means that the Ronchi images of Fig. 2 were measured at 0.07, 0.57, 1.07, 1.57, and 2.07 mm, respectively, downstream of the paraxial image plane.

3. Numerically simulating Ronchigrams

The simulation of the beam propagation from an exit pupil to a detector, as schematically described in Fig. 1, is carried out by dividing the total propagation into four regions. 1) First a converging quadratic phase wave with the aberrations retrieved from the experimental data is assumed at the exit pupil of the lens under test and this beam is propagated to the paraxial image plane (PIP). The central radius of curvature of the quadratic phase wave is equal to the distance from the pupil to the PIP. Since it is equal to the propagation distance, the quadratic phase term is cancelled off by the Fresnel diffraction integral and this cancellation leaves the initial field with just the aberrations. 2) The beam is propagated from the PIP to the Ronchi ruling (RR), in which plane we multiply the beam by the binary ruling transmissivity. 3) From RR the beam is propagated to the imaging lens (IL), where we multiply by the complex transmissivity of the lens. 4) After the IL the beam is propagated to the detector. In order to minimize the required sampling to avoid aliasing, different numerical strategies were used for each region when computing the propagation integrals [2,10]. The initial beam sampling is also adjusted so that we directly obtain a sampling of 10.4 μm at the plane of the detector, such that no additional interpolation is needed to compare to the measurements.

The propagation in region 1) is calculated by the Fresnel diffraction integral through a single Fourier transform as [10]:

$$u_2(x,y) = \frac{e^{ikz}}{i\lambda z} e^{\frac{ik}{2z}(x^2+y^2)} \iint u_1(\alpha,\beta) e^{\frac{ik}{2z}(\alpha^2+\beta^2)} e^{-\frac{i2\pi}{\lambda z}(x\alpha+y\beta)} d\alpha d\beta, \qquad (1)$$

#129106 - $15.00 USD Received 27 May 2010; revised 10 Aug 2010; accepted 10 Aug 2010; published 16 Aug 2010

where z is the propagation distance and $k(=2\pi/\lambda)$ is the wave-vector. For the regions of 2) and 4), we used a two-step transfer function approach (paraxial angular spectrum), given by [10]

$$u_2(x, y) = u_1(x, y) * h_{12}(x, y; z), \tag{2a}$$

where the transfer function is given by

$$h_{12}(x, y; z) = \frac{\exp(ikz)}{i\lambda z}\exp[i\frac{\pi}{\lambda z}(x^2 + y^2)]. \tag{2b}$$

The propagation in region of 3) is slightly more complicated. If we use Eq. (1) from the RR to the IL, we would end with a sampling at the detector that varies with the longitudinal position of the Ronchi ruling, which is not true in reality. To avoid further interpolation we divide the propagation integral from the RR to the IL into two propagations. First we propagate the field modified by the ruling back from the RR to the PIP by the two-step transfer function approach, Eq. (2). Notice that the function resulting at this point is an intermediate mathematical result that bears no physical significance. This operation is followed by another propagation from PIP to IL by a Fresnel integral, Eq. (1). This takes more execution time, but it keeps the sampling constant at the plane of the detector for different positions of the Ronchi ruling. The full propagation is executed through a total of 8 Fourier transforms to simulate a Ronchigram at the plane of detector. The inputs to the calculation are the wavelength, F/#, diameter of the exit pupil, the number of pixels to sample the exit pupil, the location of the ruling with respect to the paraxial image plane of the system, vertical/horizontal ruling's period, offset of the ruling, focal length of the imaging lens, distances from the ruling to the imaging lens, and from the imaging lens to the detector, and a set of third-order Zernike polynomial coefficients for the aberrated wave front.

For the numerical simulation, the F/# of the system was fixed at 5.24 and we used 1024 by 1024 pixels for the Fourier transform arrays. The circular pupil is assumed to be uniform amplitude and the phase deviation from a sphere is given by the set of third-order Zernike polynomial coefficients, a_4=–0.0262, a_5=0.0025, a_6=–0.2086, a_7=–0.0095, and a_8=2.1647, that were retrieved from the experimental data. The coefficient a_3 is given 6.4941 to set the system with a ruling at the PIP initially and all other higher order coefficients were ignored. At the edge of the aperture we calculated the partial area of overlap with a square pixel and assigned the amplitude to this fractional value. This smoothed the circular pupil edge, reducing aliasing artifacts and increasing the simulation accuracy. We used 457 pixels for the circular pupil diameter to set the sampling scale at the plane of detector as 10.4 μm, which matches the physical size of the pixels in the CMOS camera that was used in this work. The radius of Airy disk is 4.061 μm and the sampling scale at the paraxial image plane is 1.486 μm, indicating that the field sampling is large enough to prevent aliasing.

In order to check the validity of the quantitative Ronchigram analysis, we simulated Ronchigrams as a function of the ruling's location with respect to the PIP and compared them with the measured ones. The increment of the location was set as 0.05 mm for visual comparison. The comparison was carried out based on the width of the central bright fringe and the distance between the next bright fringes on both sides of the central fringe. According to the 3rd-order aberration theory, they are linearly proportional to the defocus or the distance from the PIP to ruling [11]. The best match was obtained for distances 0.00, 0.5, 1.0, 1.5, and 2.0 mm, respectively, away from the PIP. They are shown in Fig. 2(f) thru 2(j). In addition, Fig. 4 shows equivalent images for the horizontal ruling.

#129106 - $15.00 USD Received 27 May 2010; revised 10 Aug 2010; accepted 10 Aug 2010; published 16 Aug 2010

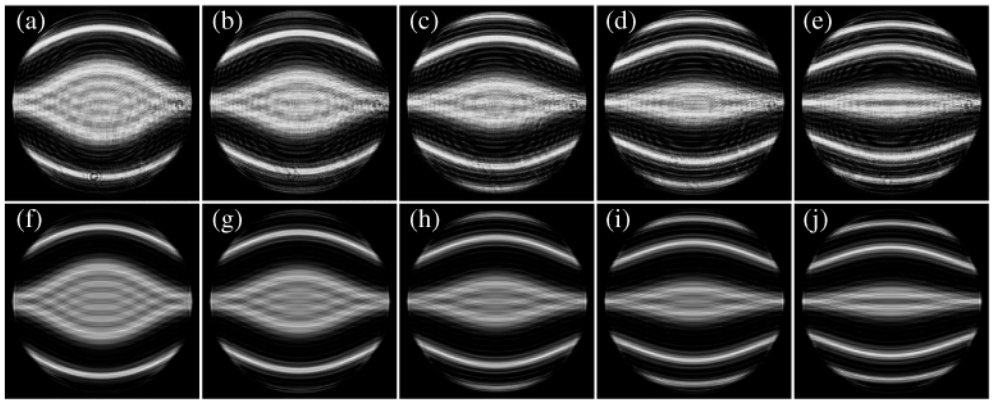

Fig. 4. π-phase Ronchigrams with horizontal ruling at (a) 13.00, (b) 13.50, (c) 14.00, (d) 14.50, and (e) 15.00 mm of the longitudinal translation stage and (f) thru (j) are their corresponding simulated images. All images are cropped to 512 by 512 pixels from the original sizes.

The discrepancy between the locations in simulations and the locations determined by Ronchigram analysis is 0.07 mm, which is comparable to the fact that the simulated images were computed with 0.05 mm increments on the position of the ruling, and to the fact that the uncertainty of the locations determined from the data analysis is also 0.05 mm. In the numerical simulation, we assumed the imaging lens as an ideal thin lens and ignored the noise and reflection artifacts. We further assumed that the paraxial image plane of the lens under test is coincident with the primary focal point of the imaging lens, which is difficult to measure accurately and cannot be guaranteed. To this extent we have simulated different combinations of distances to the imaging lens and to the detector, and found that although the overall size of the Ronchigram is modified, the structure in the pattern remains visually indistinguishable. Despite the potential inaccuracies in these parameters including an uniform amplitude for the pupil field, the overall agreement between the simulated and measured Ronchigrams is excellent. Even the fine low-contrast structures in the dark space were found in good agreement, as shown in Fig. 5, which shows the upper left quadrant of Fig. 2(b) and its corresponding simulated Ronchigram in their original sizes.

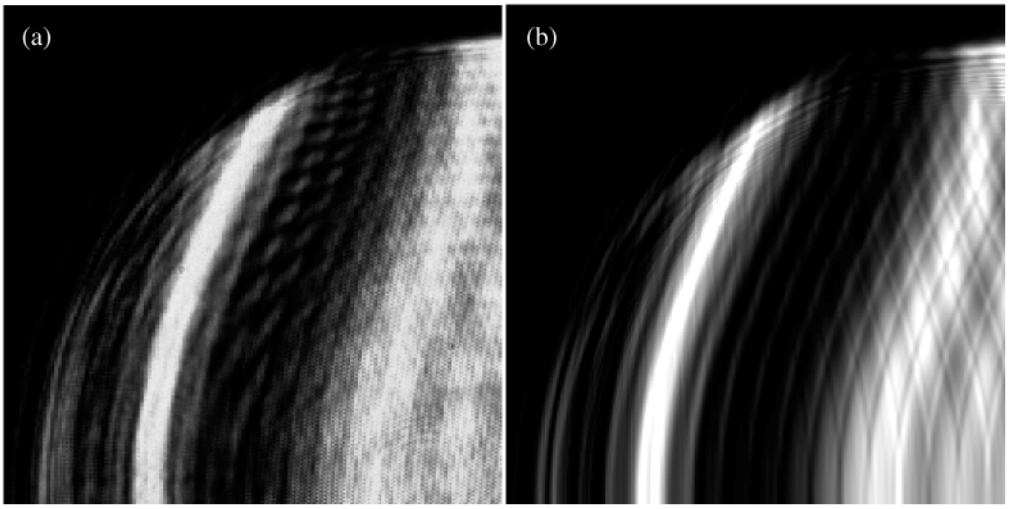

Fig. 5. Upper left quadrants of (a) Fig. 2(b) and (b) its corresponding simulated image in their original sizes. For better visualization, in the simulation the intensity was saturated by 40%.

#129106 - $15.00 USD Received 27 May 2010; revised 10 Aug 2010; accepted 10 Aug 2010; published 16 Aug 2010

We obtained an excellent agreement in both images and parametric values. This simulation requires many experimental parameters that were obtained through the Ronchigram analysis, namely, the wavefront aberrations, the system *f*-number and the location of the Ronchi ruling, which speaks favorably of both the accuracy of the numerical simulation and the parameters retrieved from the experimental Ronchigram analysis. This agreement over the set of Ronchigrams also indicates the accuracy of the rather complicated process for the numerical simulation.

4. Summary

We have validated the quantitative Ronchigram analysis with a detailed numerical simulation of propagation through our experimental setup, and shown that the parameters determined by the Ronchi test are capable to reproduce, in a great detail the measured Ronchigrams. This agreement confirms the values of the parameters obtained from Ronchigram quantitative analysis, such as F/#, the relative locations for the ruling with respect to the paraxial image point, and wavefront aberrations.

The numerical propagation additionally provides a useful framework to study in detail the effects of noise and accuracy and range of this wavefront sensing technique, with the possibility to explore several experimental variations such as grating period, optimal distance to the paraxial image plane, etc.

Furthermore, with some analogy to our experimental approach, phase retrieval techniques that perturb the beam by translating an object in the path of the beam are currently being applied to x-ray beam characterization [2]. A direction of further work could be to apply phase retrieval methods to the Ronchi test data, since with the Ronchi test we can retrieve all parameters needed for the numerical modeling of the data then it is feasible to think about applying phase retrieval as a refinement strategy for the wavefront estimation.

Acknowledgments

Thanks to James R. Fienup for helpful discussions. This work was supported by Basic Science Research Program through the National Research Foundation of Korea (NRF) funded by the Ministry of Education, Science and Technology (2009-0074964).

#129106 - $15.00 USD Received 27 May 2010; revised 10 Aug 2010; accepted 10 Aug 2010; published 16 Aug 2010